Journal of Engg. Research **Vol. 4 No. (4) December 2016** pp. 46-65

التوليف، والتوصيف والتدهور الحراري الحركي لبولي (3-اكتيلكومارين-7-YL-ميتاكريليت) ومركبات النانو العضوية

***عدنان كورت و**مورات كوكا**

*قسم الكيمياء، كلية الآداب والعلوم، جامعة اديامان، اديامان، تركيا

**قسم الكيمياء الصيدلانية، كلية الصيدلة، جامعة اديامان، اديامان، تركيا

الخلاصة

كومارين جديدة تم توليفها من (3-acetylcoumarin-7-YL – ميتاكريليت)، وبولي (ACMA)، ومكونات النانو لها مع محتويات مختلفة من organoclay تم تركيبها وهي مميزة بالرموز XRD، ^{1}H-NMR، FTIR و TGA. تحليل الأشعة السينية أظهر أن تشتت الطين في البوليمر تسبب في تقشر السلوك. تمت دراسة تأثير محتوى organoclay على التوازن الحراري للمواد متناهية الصغر عن طريق التحليل الوزني الحراري (TGA). وقد زاد التوازنات الحرارية للمواد المتناهية في الصغر nanocomposites عن طريق تحميل الطين في مصفوفة البوليمر. وظهر أن بمركب متناهي في الصغر يحتوي على 4% بالوزن من ال organoclay يحدث أفضل استقرار حراري (319 درجة مئوية) عند فقدان وزن بنسبة 10%. وقد تم التحقيق من التحليل الحركي الحراري ل nanocomposites بطرق كيسنجر ومعاطف–ريدفيرن. وبإدخال مرحلة الطين في البوليمر المتجانس تم زيادة طاقة التنشيط من 185.39 كيلو جول / مول إلى 264.30 كج / مول. آلية رد الفعل الفعلية للبولي (ACMA) و nanocomposites organoclay قد أطاعت التباطؤ في آليات نشر الأبعاد (D_n).

Synthesis, characterization and thermal degradation kinetics of poly(3-acetylcoumarin-7-yl-methacrylate) and its organoclay nanocomposites

Adnan Kurt* and Murat Koca**

**Department of Chemistry, Faculty of Arts and Science, University of Adiyaman, 02040, Adiyaman/Turkey*

***Department of Pharmaceutical Chemistry, Pharmacy Faculty, University of Adiyaman, 02040, Adiyaman/Turkey*

**Corresponding author: adnkurt@gmail.com*

ABSTRACT

A new coumarin derived polymer poly(3-acetylcoumarin-7-yl-methacrylate), poly(ACMA), and its nanocomposites with different contents of organoclay were synthesized and characterized by FTIR, ^{1}H-NMR, XRD and TGA. The X-ray diffraction analysis showed that the clay dispersion in the polymer matrix has exfoliated behavior. The influence of the organoclay content on the thermal stabilities of nanomaterials was studied by means of thermogravimetric analysis (TGA). Thermal stabilities of nanocomposites were increased by loading clay into the polymer matrix. The nanocomposite containing 4 wt.% organoclay showed the best thermal stability (319 °C) at 10% weight loss. Thermal decomposition kinetic analysis of nanocomposites was investigated by Kissinger and Coats-Redfern methods. Introduction of the clay phase into homopolymer increased the activation energy from 185.39 kJ/mol to 264.30 kJ/mol. The actual reaction mechanism of pure poly(ACMA) and its organoclay nanocomposites obeyed deceleration type dimensional diffusion mechanisms (D_n).

Keywords: Activation energy; characterization; coumarin nanocomposites; synthesis; thermal decomposition kinetics.

INTRODUCTION

Coumarins are belonging to polyphenolic compounds. The synthesis of coumarins and their derivatives has maintained its importance for many years, as a large number of natural products contain this heterocyclic nucleus, leading their biological activities (Chaudhary & Datta, 2014). Coumarin-derived polymers have also been synthesized by some researchers recently. These polymers exhibit significant properties, e.g., antibacterial, antibiotic, antimycotic, antiviral, antitumor, antifungal, antioxidant and biological marking (Soine, 1964; Pratibha & Shreeya, 1999; Patonay *et al.,* 1984;

Shaker, 1996; Emmanuel-Giota *et al.,* 2001; Nofal *et al.,* 2000; Srivastava *et al.,* 2012). Besides, they are widely used as materials in various industrial applications such as electro-optics, organic-inorganic hybrids, liquid crystals, light storage-energy transfer materials, and biochemical substances (Brun *et al.,* 2004; Zhao *et al.,* 2006; Jackson *et al.,* 2001; Kim *et al.,* 2006; Tian *et al.,* 2004).

To improve physical, chemical or mechanical properties of polymer composites as compared to macro- and micro-composites, polymer nanocomposites have been successfully used for both science and industrial applications in recent years (Krishna & Pugazhenthi, 2011). They are defined as the combination of polymer matrix and the additives having nanometer dimensions (Achilias *et al.,* 2008). Various polymer nanocomposites have been developed using different types of nanofillers such as nanoclays, carbon nanotubes and metal nanoparticles. In these nanofillers, clay is quite much preferred for the synthesis of polymer nanocomposites as it is cheap, easily available, and environment-friendly material (Panwar *et al.,* 2011). Therefore, polymer/clay nanocomposites have been extensively studied recently to achieve various excellent properties like optical, mechanical, thermal stability and flame retardancy, magnetic, electrical, gas permeation and enhanced modulus (Fujimori *et al.,* 2008; Jang *et al.,* 2005; Caruso *et al.,* 2001; Nazarenko *et al.,* 2007; Shia *et al.,* 1998). These properties are strongly dependent on the extent of separation of the silica layers of the clay particles (Lee *et al.,* 2006).

Investigation of the thermal decomposition process of polymeric materials is compulsory for many applications and provides more specific information regarding their internal structures (Achilias *et al.,* 2008; Wilkie, 1999). For this purpose, thermogravimetric analysis (TGA) is a common experimental technique used to determine the thermal decomposition parameters of polymeric materials. Although the thermal behaviors of polymer–clay nanocomposites or their thermal decomposition kinetics have been studied extensively, nearly all those nanocomposites are based on the commercially important polymers (Krishna & Pugazhenthi, 2011; Achilias *et al.,* 2008; Jang *et al.,* 2005). On the other hand, there are only a few studies on the investigation of thermal characteristics of coumarin containing polymers (Essaidi *et al.,* 2013; Erol *et al.,* 2010; Zhang *et al.,* 2008). In this point, it seems that no attention has been paid for the preparation and investigation of thermal degradation kinetics of coumarin containing polymers/organoclay nanocomposites according to our literature knowledge. Therefore, the primary aim of this study is the synthesis, characterization and investigation of the thermal degradation kinetics of novel poly(3-acetylcoumarin-7-yl-methacrylate) homopolymer and its organoclay nanocomposites. Another important aim of this study is to investigate the influence of adding organoclay on the thermal decomposition kinetic parameters and solid state decomposition mechanisms of poly(3-acetylcoumarin-7-yl-methacrylate)/organoclay nanocomposites. On the

basis of these aims, the influence of the content of organoclay on the thermal stabilities of nanomaterials is studied by means of thermogravimetric analysis (TGA) under non-isothermal heating conditions.

EXPERIMENTAL

Materials

3-acetyl-7-hidroxycoumarin, methacryloil chloride, anhydrous $MgSO_4$, K_2CO_3, chloroform, tetrahydrofuran (THF), N,N-dimethylformamide (DMF) were purchased from Sigma-Aldrich. Benzoyl peroxide (BPO) was obtained from Merck, and it was purified by dissolving in chloroform and recrystallizing from ethanol. Nanomer® I.28E (25-30 wt.% trimethyl stearyl ammonium) was purchased from Sigma–Aldrich, which used as organomodified clay (OMMT).

Sythesis of 3-acetylcoumarin-7-yl-methacrylate (ACMA) monomer

3-acetyl-7-hidroxycoumarin was synthesized as starting reagent of monomer. Therefore, a mixture of 2,4-dihydroxybenzaldehyde (2.762 g, 0.02 mol), ethyl acetoacetate (2.603 g, 0.02 mol) and piperidine as catalyst (three drops) in acetone (50 mL) were refluxed for 2 h. After completion of the reaction, the product mixture was precipitated in methanol, filtered, and vacuum dried. Then, 3-acetyl-7-hidroxycoumarin (2.042 g, 0.01 mol), K_2CO_3 (1.382 g, 0.01 mol) and THF (25 mL) were added to a three-necked round bottom flask, and the mixture was cooled to room temperature. The solution of methacryloyl chloride (1.045 g, 0.01 mol) in THF (25 mL) were added dropwise to the mixture, and stirred at room temperature for 12 h. After that, THF was evaporated, organic phase was dissolved in chloroform and extracted with dilute (5%) KOH aqueous solution several times. Finally, the monomer extracts were collected and dried over anhydrous $MgSO_4$, filtered, and the solvent was evaporated in a vacuum. The synthesis of monomer was shown in Scheme 1.

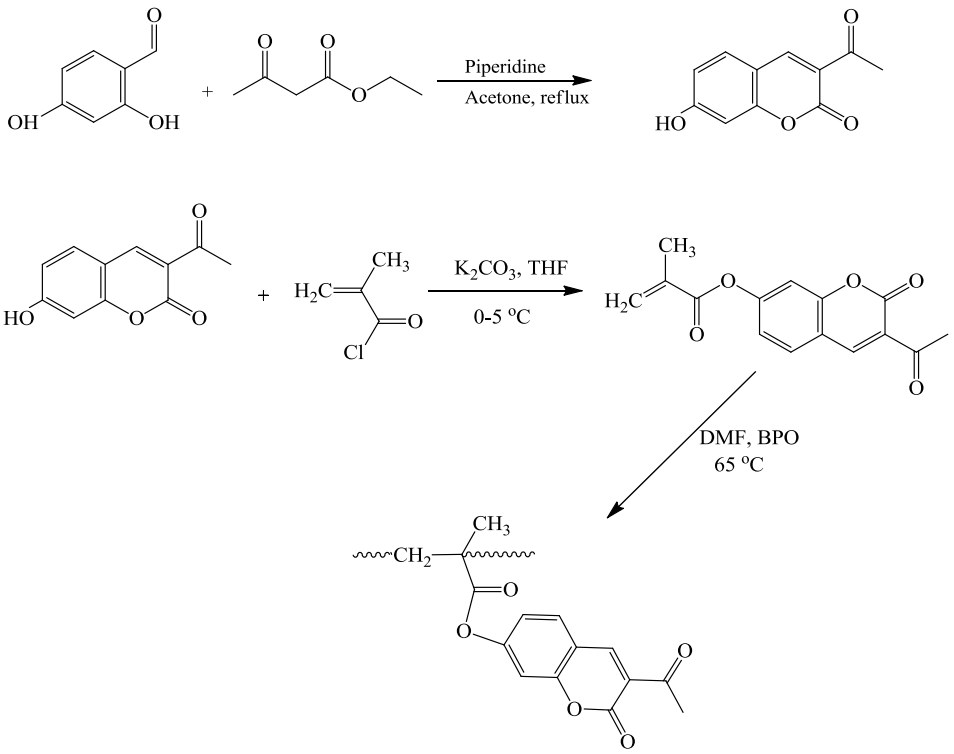

Scheme 1. Synthesis of poly(3-acetylcoumarin-7-yl-methacrylate)

Synthesis of poly(ACMA)/OMMT nanocomposites

Poly(3-acetylcoumarin-7-yl-methacrylate) was synthesized by free radical polymerization using 2.0 g of ACMA, 6.0 mL of N,N-dimethylformamide (DMF) as solvent and 0.020 g (1 wt.% of the monomer) of benzoyl peroxide as initiator at 65 ºC ± 1 ºC for 6 h. The polymer was purified by twice repeated dissolution/ precipitation in chloroform/methanol, isolated by filtration, and dried overnight in a vacuum oven at 40 ºC. Poly(ACMA)/OMMT nanocomposites were prepared with solution casting method. In a round bottom flask, desired amount of organoclay (2% and 4%) was dispersed in 3 mL of DMF and stirred by magnetic stirrer at 60 °C for 24 h. During this period, 0.5 g poly(ACMA) was dissolved in 3 mL of DMF at room temperature in another flask. Then, poly(ACMA)/DMF solution was added gradually into the organoclay/DMF suspension. Finally, the mixture was stirred for 24 h with a magnetic stirrer at room temperature. The polymer/organoclay mixtures were then precipitated in excess ethyl alcohol to isolate from DMF solvent. Poly(ACMA)/ OMMT nanocomposites were first air-dried for 12 h and finally, they were kept in air oven at 40 °C for 24 h for complete removal of the precipitator.

Instrumental techniques

Nuclear magnetic resonance spectra (^{1}H-NMR) were recorded on a Bruker 300 Mhz Ultrashield TM instrument at room temperature using $CDCl_3$ (for monomer) and $CDCl_3$/DMF (for polymer) solvents and TMS as an internal standard. A Perkin Elmer Spectrum 100 was used to obtain the infrared spectra of the nanocomposites. XRD patterns were recorded under air at room temperature using Rigaku RadB-DMAX II X-Ray Diffractometer equipped with a Cu-Kα radiation (λ = 0.15418 nm) and Ni filter. The thermogravimetric analysis was conducted on a Seiko SII 7300 TG/DTA under nitrogen flow from 25 °C to 500 °C at the heating rates of 5 °C/min, 10 °C/min, 15 °C/min and 20 °C/min. A Perkin Elmer DSC 8000 was used to examine the glass transition temperature of the nanocomposites. Samples were heated from 25 °C to 200 °C at a rate of 20 °C/min under nitrogen atmosphere.

RESULTS AND DISCUSSION

FTIR spectra of 3-acetylcoumarin-7-yl-methacrylate (ACMA) and its homopolymer poly(ACMA) were shown in Figure 1(a,b). Also, the most characteristic FTIR band assignments of ACMA and poly/ACMA) were given in Table 1. In the frequency region of C=C stretching, only the absorption band at 1608 cm^{-1} for aromatic C=C stretching was observed, whereas the aliphatic C=C stretching was disappeared. This disappearance is one of the main evidences that the homopolymerization of ACMA is accomplished by free radical polymerization method.

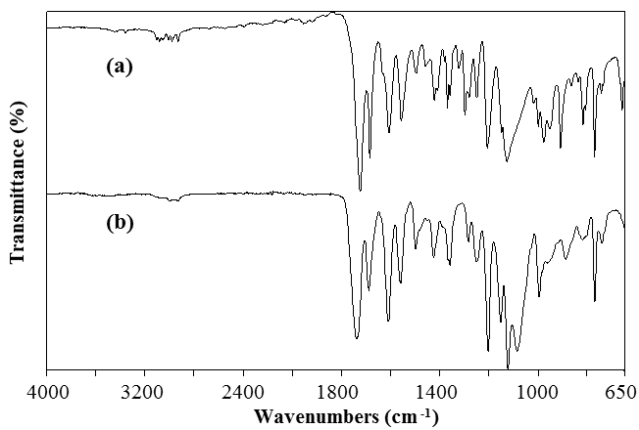

Fig. 1. FTIR spectra of a) ACMA monomer, b) poly(ACMA) homopolymer

Table 1. The most characteristic FTIR band assignments of ACMA and poly/ACMA)

Compound	Frequency (cm^{-1})	Assignment
ACMA monomer (Fig. 1a)	3108-3013	Aromatic C-H stretching vibration
	2979-2856	Aliphatic C-H stretching vibration
	1738, 1724 and 1683	Methacrylic ester, ketone and lactone carbonyl vibrations
	1631 and 1605	Aliphatic and aromatic C=C stretching vibrations
Poly(ACMA) homopolymer (Fig. 1b)	3118-3002	Aromatic C-H stretching vibration
	2992-2853	Aliphatic C-H stretching vibration
	1736, 1725 and 1689	Methacrylic ester, ketone and lactone carbonyl vibrations,
	1608	Aromatic C=C stretching

^{1}H-NMR spectra and the chemical shift assignments of ACMA and poly(ACMA) were given in Figure 2(a,b) and Table 2, respectively. In Figure 2(b), the resonances at 1.6 ppm and 2.7 ppm were attributed to methyl protons of methacrylate group and coumarin ring, respectively. Both singlets at 5.8 ppm and 6.4 ppm assigned to vinyl protons of ACMA monomer were disappeared with polymerization. These protons were seen as new backbone protons at the chemical shift region 1.4 ppm - 1.7 ppm. The multiplet resonance absorptions between 7.1 ppm and 8.5 ppm were characteristic for aromatic protons on coumarin ring. The other signals in Figure 2(b) were due to deuterated-DMF (8.03, 2.92, 2.75 ppm) and $CDCl_3$ (7.27 ppm) solvents.

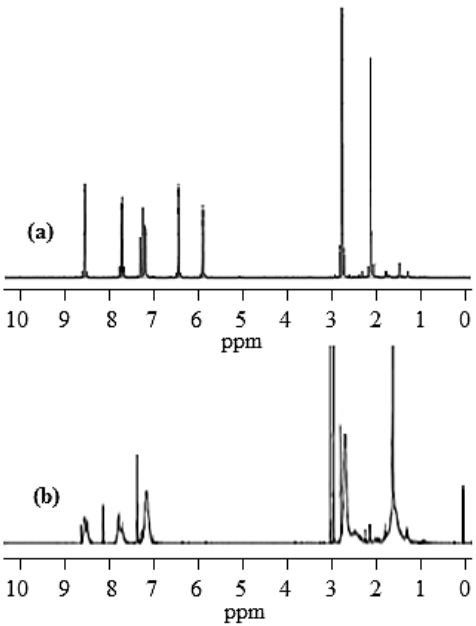

Fig. 2. ^{1}H-NMR spectra of a) ACMA monomer, b) poly(ACMA) homopolymer.

Table 2. ^{1}H-NMR assignments of ACMA and poly(ACMA)

Compound	Chemical shifts (ppm)	Assignment
ACMA monomer (Fig. 2a)	7.6 - 8.5	Aromatic protons on coumarin ring
	5.8 and 6.4	Vinyl protons
	2.1 and 2.7	Methyl protons of methacrylate group and coumarin ring
Poly(ACMA) homopolymer (Fig. 2b)	7.1 - 8.5	Aromatic protons on coumarin ring
	1.6 and 2.7	Methyl protons of methacrylate group and coumarin ring
	1.4 - 1.7	Backbone protons

XRD analysis is an effective technique to characterize the types of the layered structure of polymer/organoclay nanocomposites, intercalated and/or exfoliated, because the peak changes with the gallery height of the organoclay (Krishna & Pugazhenthi, 2011; Lee *et al.,* 2006; Fu & Qutubuddin, 2001; Fan *et al.,* 2003). In the case of intercalated nanocomposites, a XRD peak is seen at larger d-spacing than in the pristine clay, whereas in case of exfoliated structure, no peak is seen (Krishna & Pugazhenthi, 2011). The d_{001} spacing was calculated from peak positions using Bragg's law: $n\lambda = 2d \sin\theta$, where λ is the X-ray wave length (1.5418 A°).

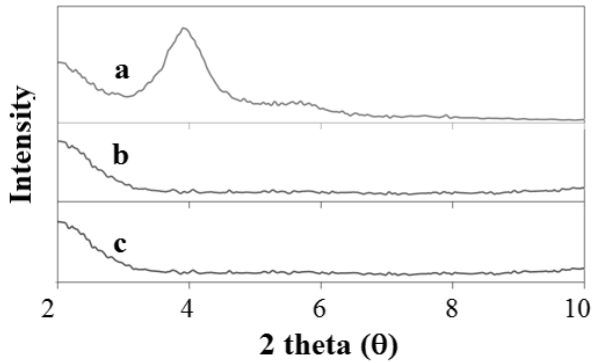

Fig. 3. XRD patterns of a) organoclay (OMMT), b) poly(ACMA)/OMMT:2%, c) poly(ACMA)/OMMT:4%

Figure 3 shows the wide-angle X-ray diffraction patterns of nanocomposites. In Figure 3(a), the diffraction peak of nanomer clay layers appears at about 3.9° corresponding to the basal spacing 2.26 nm. This indicates that the basal spacing of the modified clay is greatly influenced by the long alkyl chain and by the volume of the substituent of the intercalating agent (Zhang *et al.,* 2003). The wide-angle X-ray diffraction patterns of poly(ACMA)/OMMT nanocomposites containing 2% and 4% organoclay contents are shown in Figure 3(b,c) where there are no characteristic OMMT peaks in the testing range of 2-theta. Also, in these figures, the diffraction

peaks of the all nanocomposites are completely disappeared. These results indicate that the organoclay dispersion in the polymer matrix is exfoliated (Krishna & Pugazhenthi, 2011).

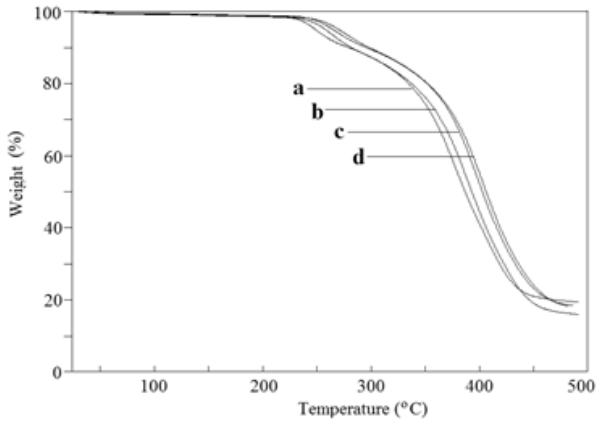

Fig. 4. TGA curves of poly(ACMA) at different heating rates a) 5 °C/min, b) 10 °C/min, c) 15 °C/min, d) 20 °C/min

Thermal degradation behaviors of poly(3-acetylcoumarin-7-yl-methacrylate)/ organoclay nanocomposites samples were determined by thermogravimetric analysis (TGA) under non-isothermal heating conditions. The dynamic experiments of degradation of nanocomposites were performed by increasing the temperature up to 500 °C at the heating rates of 5, 10, 15 and 20 °C/min in an inert atmosphere of argon. TGA curves of poly(ACMA) homopolymer and its organoclay nanocomposites at these heating rates were illustrated in Figures 4-6 and their results were given in Table 3.

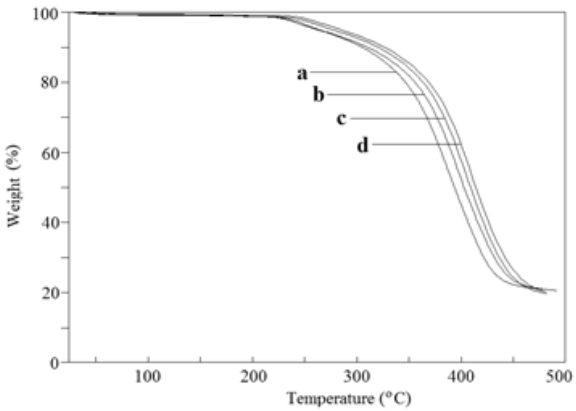

Fig. 5. TGA curves of poly(ACMA)/OMMT:2% at different heating rates a) 5 °C/min, b) 10 °C/min, c) 15 °C/min, d) 20 °C/min

Table 3. TGA data of poly(ACMA)/OMMT nanocomposites

Polymer	Heating rate (°C/min)	T_1 (°C)	T_2 (°C)	%Weight loss at 300 °C	%Weight loss at 400 °C	% residue at 500 °C
Poly(ACMA)	5	279	387	12.8	58.6	19.0
	10	281	398	12.7	55.3	16.0
	15	295	402	10.6	47.5	18.5
	20	300	406	10.3	44.8	18.3
Poly(ACMA)/OMMT:2%	5	306	394	9.3	54.7	21.8
	10	310	404	8.6	48.2	21.9
	15	319	409	7.4	43.3	19.7
	20	327	414	6.7	38.6	20.2
Poly(ACMA)/OMMT:4%	5	315	404	7.6	46.2	26.0
	10	319	412	7.3	48.5	25.6
	15	322	415	7.1	38.5	22.4
	20	329	421	6.4	33.9	24.9

T_1 and T_2: Decomposition temperatures at 10% and 50% weight loss, respectively.

As it can be seen in Figures 4-6, there is a lateral shift to higher temperatures for the initial decomposition temperatures as the heating rate is increased. The variations in the rate of heat transfer may effect to this behavior due to the short exposure time to a particular temperature at higher heating rates and the kinetics of decomposition. At higher heating rates, there is an incompatibility between the external and core heats of decomposed particles. Because the external surface of particles more heats than its core, the decomposition reactions of external surface occur at higher temperatures by increasing the heating rates (Aboulkas & El Harfi, 2008).

To determine the thermal stabilities of nanocomposites, TGA curves at heating rate of 10 °C/min were compared with each other, and thermograms were also shown in Figure 7. The weight loss curve in Figure 7(a) showed that decomposition of poly(ACMA) took place in one stage at ≈15% weight loss area which can be attributed to the formation of volatile hydrocarbons in the first decomposition temperature range up to approximately 280 °C (Koca *et al.,* 2012).

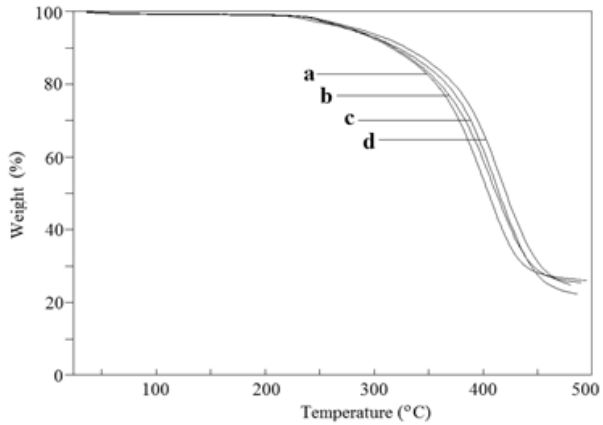

Fig. 6. TGA curves of poly(ACMA)/OMMT:4% at different heating rates a) 5 °C/min, b) 10 °C/min, c) 15 °C/min, d) 20 °C/min

On the other hand, the decomposition of poly(ACMA)/OMMT clay nanocomposites took place in one stage at ≈5% weight loss area about to 260 °C as shown in Figure 7(b,c). This may be reasoned by thermal decomposition of the alkyl chains of surfactant molecules present between the interlayer of organoclay. The second step of weight losses of pure poly(ACMA) and its nanocomposites appear approximately between 300 °C and 450 °C, which is attributable to decomposition of polymer chains.

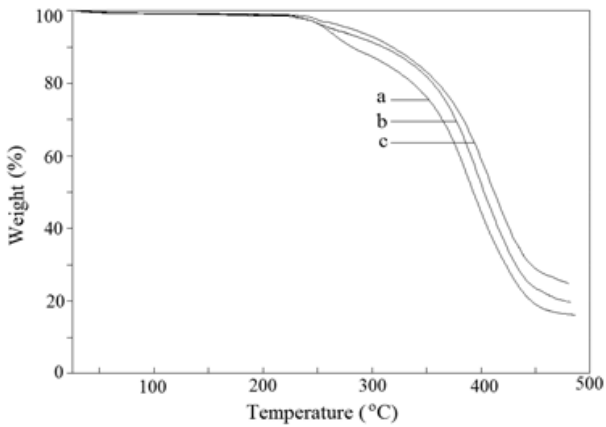

Fig. 7. TGA curves of nanocomposites at 10 °C/min heating rate: a) poly(ACMA), b) poly(ACMA)/OMMT:2%, c) poly(ACMA)/OMMT:4%

Table 3 includes a few data related to decomposition, where the peak temperatures for all samples shift to higher values with increasing heating rate. This alteration has been recorded in the case of thermal degradation of different types of polymers (Li *et al.,* 2004; Kurt, 2009; Meng *et al.,* 2007). Table 3 also clearly demonstrates that the thermal decomposition temperature of poly(ACMA)/OMMT nanocomposites

are higher than that of pure poly(ACMA) homopolymer. When the 10% weight loss and 10 °C/min heating rate were chosen for comparison, the thermal decomposition temperature for poly(ACMA) homopolymer and its nanocomposites containing 2% and 4% organoclay were found to be 281°C, 310 °C and 319 °C, respectively. The best thermal stability was observed for the nanocomposite containing 4% OMMT at 319 °C. Increasing of decomposition temperature to higher values with organoclay loading has been reported in literature (Vyazovkin *et al.,* 2004; Doh & Cho, 1998; Zanetti *et al.,* 2004; Thellen *et al.,* 2005; Lepoittevin *et al.,* 2002).

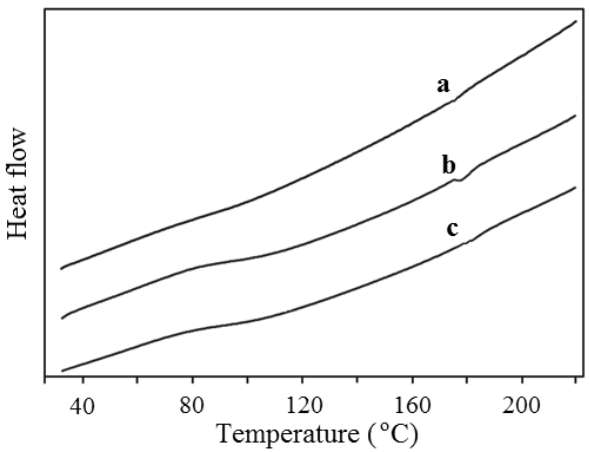

Fig. 8. DSC curves of nanocomposites: a) poly(ACMA), b) poly(ACMA)/OMMT:2%, c) poly(ACMA)/OMMT:4%

The glass transition temperatures (T_g) of poly(ACMA)/OMMT nanocomposites were determined by DSC technique, and the results were shown in Figure 8. DSC curves of nanocomposites showed that the glass transition temperature of the nanocomposites increased relatively to the pure poly(ACMA). The Tg of poly(ACMA) homopolymer and its nanocomposite samples containing 2% and 4% of clay were determined as 176 °C, 178 °C and 181 °C, respectively. It was observed that the glass transition temperature of nanocomposites was 2–5 °C higher than that of pure poly(ACMA). This may be because the movement of poly(ACMA) homopolymer chains are prevented by the sheets of the clay. The segmental motions of the polymer chains are restricted at the organic-inorganic interface due to the confinement of the poly(ACMA) chains between the silicate layers and the silicate surface polymer interaction (Zhang *et al.,* 2003; Krishna & Pugazhenthi, 2011; Huang *et al.,* 2001). In general, this improvement ratio at the transition glass temperature for polymer/organoclay nanocomposites seems approximately 2-7 °C in literature (Zidelkheir *et al.,* 2006; Wang *et al.,* 2004).

Table 4. Algebraic expressions for g(α) for the most frequently used mechanisms of solid state processes

Symbol	g(α)	Solid state processes
Sigmoidal curves		
A_2	$[-\ln(1-\alpha)]^{1/2}$	Nucleation and growth (Avrami equation 1)
A_3	$[-\ln(1-\alpha)]^{1/3}$	Nucleation and growth (Avrami equation 2)
A_4	$[-\ln(1-\alpha)]^{1/4}$	Nucleation and growth (Avrami equation 3)
Deceleration curves		
R_1	α	Phase boundary controlled reaction (One-dimensional movement)
R_2	$[1-(1-\alpha)^{1/2}]$	Phase boundary controlled reaction (contraction area)
R_3	$[1-(1-\alpha)^{1/3}]$	Phase boundary controlled reaction (contraction volume)
D_1	α^2	One-dimensional diffusion
D_2	$(1-\alpha)\ln(1-\alpha)+\alpha$	Two-dimensional diffusion
D_3	$[1-(1-\alpha)^{1/3}]^2$	Three-dimensional diffusion (Jander equation)
D_4	$(1-2/3\alpha)\ (1-\alpha)^{2/3}$	Three-dimensional diffusion (Ginstling-Brounshtein equation)
F_1	$-\ln(1-\alpha)$	Random nucleation with one nucleus on the individual particle
F_2	$1/\ (1-\alpha)$	Random nucleation with two nuclei on the individual particle
F_3	$1/\ (1-\alpha)^2$	Random nucleation with three nuclei on the individual particle

Decomposition reaction is expressed in terms of order based reaction kinetics. Generally, the kinetic equation of the process can be written as Equation (1) (Vyazovkin, 2006):

$$\frac{d\alpha}{dt} = k(T)f(\alpha) \tag{1}$$

where α represents the extent of reaction, which can be determined from TGA runs as a fractional mass loss, *t* is time, k(T) is a temperature-dependent rate constant, and f(α) denotes the particular reaction model, which describes the dependence of the reaction rate on the extent of reaction. If an Arrhenius type expression is used to describe the temperature dependence of k(T), then Equation (1) yields:

$$\frac{d\alpha}{dt} = A\ exp\left(-\frac{E}{RT}\right)f(\alpha) \tag{2}$$

with A and E being the pre-exponential factor and the activation energy, respectively. Integrating this equation gives the integral function of conversion, g(α), as follows:

$$g(\alpha) = \int_0^{\alpha_p} \frac{d\alpha}{f(\alpha)} = \frac{A}{\beta} \int_0^{T_p} e^{-\frac{E}{RT}} \, dT \tag{3}$$

In case of thermal degradation of materials, two degradation processes can be seen, which is a sigmoidal function or a deceleration function (Hatakeyama & Quinn, 1994; Criado *et al.,* 1989; Ma *et al.,* 1991). Different expressions of integral function of conversion for thermally stimulated solid-state reaction mechanisms are listed in Table 4. In order to estimate the thermal degradation mechanism of nanomaterials, these functions can be applied to thermogravimetry (Zivkovic & Sestak, 1998). In the present investigation, the kinetic information was evaluated from dynamic experiments by means of different methods.

Kissinger method has widely been used in the investigation of the activation energy of solid-state reactions as seen in the decomposition processes of polymers (Kissinger, 1957). Kissinger equation is given as:

$$\ln\left(\frac{\beta}{T_{max}^2}\right) = \left\{ \ln\frac{AR}{E} + \ln\left[n(1 - \alpha_{max})^{n-1}\right] \right\} - \frac{E}{RT_{max}} \tag{4}$$

where T_{max} is the temperature corresponding to the maximum reaction rate where first derivative of TGA data is maximum, β is the heating rate in °C/min, α_{max} is the maximum conversion at T_{max}, A is the pre-exponential factor, R is the ideal gas constant, n is the reaction order of thermal degradation, and E is the activation energy. The temperature corresponding to the maximum reaction rate (T_{max}) at heating rates of 5, 10, 15 and 20 °C/min determined from derivative thermogravimetry (DTG) are 377.7, 389.4, 398.2, and 403.2 °C for poly(ACMA) homopolymer; 386.0, 397.1, 403.8, and 411.4 °C for nanocomposite containing 2% organoclay; and 396.8, 407.3, 411.2, and 416.5 °C for nanocomposite containing 4% organoclay, respectively. These results show that there is a lateral shift to higher temperatures for the temperature corresponding to the maximum reaction rate as the heating rate is increased, and also by loading organoclay.

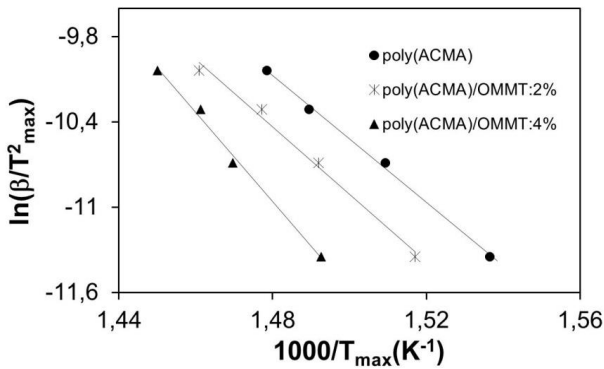

Fig. 9. Kissinger plots of a) poly(ACMA), b) poly(ACMA)/OMMT:2%, c) poly(ACMA)/OMMT:4%

The plots of $\ln(\beta/T^2_{max})$ versus $1000/T_{max}$ for homopolymer and its nanocomposites were illustrated in Figure 9. By fitting these plots to a straight line, the decomposition activation energies are obtained from a slope of $-E/R$, which are 185.39 kJ/mol, 197.10 kJ/mol and 264.30 kJ/mol for poly(ACMA) homopolymer and for nanocomposites of 2% and 4% organoclay, respectively. These results conclude that the poly(ACMA)/OMMT clay nanocomposites have higher activation energies and thermal resistance than pure poly(ACMA). The decomposition activation energies of nanocomposites were also increased with organoclay loading.

Table 5. Activation energies of different kinetic mechanisms using Coats-Redfern method for poly(ACMA) homopolymer

	5 ºC/min		**10 ºC/min**		**15 ºC/min**		**20 ºC/min**	
Mechanism	***E*** **(kJ/mol)**	***r***	***E*** **(kJ/mol)**	***r***	***E*** **(kJ/mol)**	***r***	***E*** **(kJ/mol)**	***r***
A_2	38.47	0.9962	34.44	0.9915	38.80	0.9931	39.05	0.9906
A_3	22.37	0.9947	19.68	0.9881	22.50	0.9906	22.67	0.9873
A_4	14.32	0.9925	12.30	0.9824	14.35	0.9866	14.47	0.9820
R_1	83.32	0.9961	75.56	0.9922	84.20	0.9934	84.70	0.9912
R_2	85.05	0.9966	77.15	0.9930	85.95	0.9941	86.47	0.9921
R_3	85.61	0.9968	77.67	0.9932	86.53	0.9943	87.05	0.9923
D_1	176.55	0.9966	161.04	0.9933	178.58	0.9942	179.60	0.9923
D_2	178.78	0.9969	163.10	0.9937	180.85	0.9946	181.89	0.9928
D_3	181.05	0.9972	165.19	0.9941	183.15	0.9950	184.21	0.9932
D_4	179.53	0.9970	163.79	0.9939	181.62	0.9948	182.66	0.9929
F_1	86.75	0.9971	78.72	0.9937	87.69	0.9947	88.22	0.9928
F_2	-2.94	0.8756	-3.51	0.9396	-3.11	0.9016	-3.06	0.9138
F_3	3.94	0.7411	2.83	0.6899	3.88	0.7628	3.98	0.7996

Coats–Redfern method can be used to determine the most probable thermal degradation mechanisms of poly(ACMA)/OMMT nanocomposites. Coats & Redfern, (1964) used an asymptotic approximation for the resolution of Equation (3). Thus, following equation is obtained:

$$\ln \frac{g(\alpha)}{T^2} = \ln \frac{AR}{\beta E} - \frac{E}{RT} \quad (5)$$

where g(α) is the integral function, the expression of which depends on the kinetic model of the occurring reaction. If the correct g(α) is used, a plot of $\ln[g(\alpha)/T^2]$ against 1000/T should give a straight line. Thus, the values of the apparent activation energy E for each heating rate in the conversion range can be determined.

In order to determine the decomposition mechanisms of both coumarin homopolymer and its clay nanocomposites agree better with, we have compared the activation energies obtained by Kissinger methods because it doesn't require previous knowledge of the reaction mechanism for determining of activation energy (Ma *et al.,* 1991). The decomposition activation energies for thermal decomposition of poly(ACMA) homopolymer and its clay nanocomposites at different heating rates were summarized in Tables (5-7).

Table 6. Activation energies of different kinetic mechanisms using Coats-Redfern method for poly(ACMA)/OMMT:2% nanocomposites

	5 ºC/min		10 ºC/min		15 ºC/min		20 ºC/min	
Mechanism	***E*** **(kJ/mol)**	***r***	***E*** **(kJ/mol)**	***r***	***E*** **(kJ/mol)**	***r***	***E*** **(kJ/mol)**	***r***
A_2	54.94	0.9929	51.19	0.9952	56.24	0.9867	58.60	0.9935
A_3	33.26	0.9912	30.72	0.9939	34.04	0.9837	35.58	0.9921
A_4	22.42	0.9890	20.49	0.9921	22.94	0.9797	24.07	0.9902
R_1	115.29	0.9927	108.21	0.9949	118.05	0.9871	122.72	0.9937
R_2	117.65	0.9935	110.42	0.9956	120.47	0.9881	125.20	0.9942
R_3	118.42	0.9937	111.14	0.9958	121.26	0.9884	126.01	0.9943
D_1	240.83	0.9934	226.77	0.9955	246.61	0.9883	256.04	0.9943
D_2	243.85	0.9938	229.61	0.9958	249.71	0.9889	259.23	0.9945
D_3	246.92	0.9942	232.50	0.9962	252.87	0.9894	262.47	0.9948
D_4	244.87	0.9940	230.57	0.9960	250.76	0.9890	260.31	0.9946
F_1	119.96	0.9941	112.60	0.9961	122.85	0.9890	127.64	0.9946
F_2	-0.78	0.2489	-1.45	0.5287	-0.78	0.2760	-0.62	0.1095
F_3	8.53	0.9034	7.32	0.8700	8.79	0.9186	9.20	0.8646

From the analyses of different g(α) kinetic models, it could be found that the activation energy values of homopolymer and its clay nanocomposites correspond to a deceleration type dimensional diffusion mechanisms (D_n), which have best agreement with the values obtained by Kissinger method. When it was considered for homopolymer, at the heating rate of 20 °C/min, the activation energy corresponding to D_3 mechanism was 184.21 kJ/mol (Table 5), which was very close to that of 185.39 kJ/mol obtained by Kissinger method. Thus, three-dimensional diffusion mechanism of D_3 can be the probable thermodegradation kinetic mechanism of poly(3-acetylcoumarin-7-yl-methacrylate) homopolymer. Table 6 and 7 show the activation energies for the polymer nanocomposites of containing 2% and 4% organoclay determined by Coats Redfern method, respectively. In Table 6, the activation energy value of 226.27 kJ/mol obtained at the heating rate of 10 ºC/min corresponding to a deceleration type of D_1 mechanism is in good agreement with the value obtained with the Kissinger method, which is 197.10 kJ/mol. In Table 7, the best agreement with the activation energy of Kissinger method was also determined for D_n reaction mechanisms in all heating rates. In particular, the activation energy calculated for D_3 process at a heating rate of 10 °C/min was 258.49 kJ/mol, which is in good agreement with the value obtained by Kissinger method that of 264.30 kJ/mol for 4% organoclay nanocomposite.

Table 7. Activation energies of different kinetic mechanisms using Coats-Redfern method for poly(ACMA)/OMMT:4% nanocomposites

	5 ºC/min		**10 ºC/min**		**15 ºC/min**		**20 ºC/min**	
Mechanism	***E*** **(kJ/mol)**	***r***	***E*** **(kJ/mol)**	***r***	***E*** **(kJ/mol)**	***r***	***E*** **(kJ/mol)**	***r***
A_2	54.90	0.9908	57.69	0.9840	52.63	0.9633	54.56	0.9871
A_3	33.18	0.9886	35.02	0.9806	31.62	0.9548	32.87	0.9841
A_4	22.32	0.9857	23.69	0.9761	21.11	0.9433	22.02	0.9799
R_1	115.37	0.9908	120.80	0.9848	111.08	0.9667	114.98	0.9880
R_2	117.74	0.9916	123.28	0.9858	113.40	0.9682	117.33	0.9887
R_3	118.51	0.9919	124.08	0.9861	114.16	0.9687	118.10	0.9889
D_1	241.16	0.9917	252.09	0.9861	232.73	0.9697	240.62	0.9891
D_2	244.19	0.9921	255.26	0.9867	235.70	0.9705	243.64	0.9895
D_3	247.28	0.9926	258.49	0.9872	238.73	0.9714	246.71	0.9899
D_4	245.22	0.9923	256.33	0.9869	236.71	0.9708	244.66	0.9896
F_1	120.06	0.9924	125.70	0.9866	115.68	0.9696	119.64	0.9894
F_2	-0.91	0.3355	-0.54	0.1337	-1.24	0.6233	-1.21	0.3916
F_3	8.43	0.9094	9.23	0.9132	7.93	0.9411	8.10	0.8726

CONCLUSIONS

A novel coumarin derived polymer poly(3-acetylcoumarin-7-yl-methacrylate) was synthesized and characterized. The X-ray diffraction analysis showed that the clay dispersion in the polymer matrix was exfoliated behavior. The influence of the content of organoclay on the thermal stabilities of nanomaterials was studied by means of TGA. Thermal stabilities of nanocomposites were increased about 29-38 °C by loading clay into the polymer matrix. Thermal decomposition kinetic analyses were investigated by Kissinger and Coats-Redfern methods. Introduction of the clay phase into homopolymer increased the activation energy from 185.39 kJ/mol to 264.30 kJ/mol. The actual reaction mechanism of poly(3-acetylcoumarin-7-yl-methacrylate) homopolymer and its organoclay nanocomposites obeyed deceleration type dimensional diffusion mechanisms (D_n).

ACKNOWLEDGEMENTS

We thank the Scientific and Technological Research Council of Turkey (TUBITAK-2209) for partial financially supporting this study.

REFERENCES

Aboulkas, A. & El Harfi, K. 2008. Study of the kinetics and mechanisms of thermal decomposition of moroccan tarfaya oil shale and its kerogen. Oil Shale, **25**:426–443.

Achilias, D.S., Karabela, M.M. & Sideridou, I.D. 2008. Thermal degradation of light-cured dimethacrylate resins Part I. Isoconversional kinetic analysis. Thermochimica Acta **472**:74-83.

Brun, M.P., Bischoff, L. & Garbay, C. 2004. A very short route to enantiomerically pure coumarin-bearing fluorescent amino acids. Angewandte Chemie International Edition, **43**:3432-3436.

Caruso, F., Spasova, M., Susha, A., Giersig, H. & Caruso, R.A. 2001. Magnetic nanocomposite particles and hollow spheres constructed by a sequential layering approach. Chemistry of Materials, **13**:109-116.

Chaudhary, R. & Datta, M. 2014. Synthesis of coumarin derivatives: A green process. European Chemical Bulletin, **3**:63-69.

Coats, A.W. & Redfern, J.P. 1964. Kinetic parameters from thermogravimetric data. Nature, **201**:68-69.

Criado, J.M., Malek, J. & Ortega, A. 1989. Applicability of the master plots in kinetic analysis of non-isothermal data. Thermochimica Acta, **147**:377-385.

Doh, J.G. & Cho, I. 1998. Synthesis and properties of polystyrene organoammonium montmorillonite hybrid. Polymer Bulletin, **41**:511-518.

Emmanuel-Giota, A.A., Fylaktakidou, K.C., Hadjipavlou-Litina, D.J., Litinas, K.E. & Nicolaides, D.N. 2001. Synthesis and biological evalution of several 3-(coumarin-4-yl)tetrahydroisoxazole and 3-(coumarin-4-yl)dihydropyrazole derivatives. Journal of Heterocyclic Chemistry, **38**:717-722.

Erol, I., Sanli, G., Dilek, M. & Ozcan, L. 2010. Synthesis and characterization of novel methacrylate copolymers based on sulfonamide and coumarine: monomer reactivity ratios, biological activity, thermal stability, and optical properties. Journal of Polymer Science Part A: Polymer Chemistry, **48**:4323-4334.

Essaidi, Z., Krupka, O. Iliopoulos, K., Champigny, E., Sahraoui, B., Salle, M. & Gindre, D. 2013. Synthesis and functionalization of coumarin-containing copolymers for second order optical

nonlinearities. Optical Materials, **35**:576-581.

Fan, X.W., Xia, C.J. & Advincula, R.C. 2003. Intercalation of polymerization initiators into montmorillonite platelets: free radical vs. anionic initiator clays. Colloids and Surfaces A: Physicochemical and Engineering Aspects, **219**:75-86.

Fu, X. & Qutubuddin, S. 2001. Polymer-clay nanocomposites: exfoliation of organophilic montmorillonite nanolayers in polystyrene. Polymer, **42**:807-813.

Fujimori, A., Ninomiya, N. & Masuko, T. 2008. Structure and mechanical properties in drawn poly(l-lactide)/clay hybrid films. Polymers for Advanced Technologies, **19**:1735-1744.

Hatakeyama, T. & Quinn, F.X. 1994. Thermal analysis. Fundamentals and applications to polymer science, Wiley, England.

Huang, J.C., Zhu, Z.K., Yin, J., Qian, X.F. & Sun, Y.Y. 2001. Poly(etherimide)/ montmorillonite nanocomposites prepared by melt intercalation: morphology, solvent resistance properties and thermal properties. Polymers, **42**:873-877.

Jackson, P.O., O'Neill, M., Duffy, W.L., Hindmarsh, P., Kelly, S.M. & Owen, G.J. 2001. An investigation of the role of cross-linking and photodegradation of side-chain coumarin polymers in the photoalignment of liquid crystals. Chemistry of Materials, **13**:694-703.

Jang, B.N., Costache, M. & Wilkie, C.A. 2005. The relationship between thermal degradation behavior of polymer and the fire retardancy of polymer/clay nanocomposites. Polymer, **46**:10678-10687**.**

Kim, C., Trajkovska, A., Wallace, J.U. & Chen, S.H. 2006. New insight into photoalignment of liquid crystals on coumarin-containing polymer films. Macromolecules, **39**:3817-3823.

Kissinger, H.E. 1957. Reaction kinetics in differential thermal analysis. Analytical Chemistry, **29**:1702-1706.

Koca, M., Kurt, A., Kirilmis, C. & Aydogdu, Y. 2012. Synthesis, characterization, and thermal degradation of novel poly(2-(5-bromo benzofuran-2-yl)-2-oxoethyl methacrylate). Polymer Engineering and Science,**52**:323-330.

Krishna, S.V. & Pugazhenthi, G. 2011. Properties and thermal degradation kinetics of polystyrene/ organoclay nanocomposites synthesized by solvent blending method: Effect of processing conditions and organoclay loading. Journal of Applied Polymer Science, **120**:1322-1336.

Kurt, A. 2009. Thermal decomposition kinetics of poly(nButMA-b-St) diblock copolymer synthesized by ATRP. Journal of Applied Polymer Science, **114**:624-629.

Lee, M.H., Dan, C.H., Kim, J.H., Cha, J., Kim, S., Hwang, Y. & Lee, C.H. 2006. Effect of clay on the morphology and properties of PMMA/poly(styrene-co-acrylonitrile)/clay nanocomposites prepared by melt mixing. Polymer, **47**:4359-4369.

Lepoittevin, B., Pantoustier, N., Devalckenaere, M., Alexandre, M., Kubies, D. & Calderg, C. 2002. Poly(epsilon-caprolactone)/clay nanocomposites by in-situ intercalative polymerization catalyzed by dibutyltin dimethoxide. Macromolecules, **35**:8385-8390.

Li, L.Q., Guan, C.X., Zhang, A.Q., Chen, D.H. & Qing, Z.B. 2004. Thermal stabilities and the thermal degradation kinetics of polyimides. Polymer Degradation and Stability, **84**:369-373.

Ma, S., Hill, J.O. & Heng, S. 1991. A kinetic-analysis of the pyrolysis of some Australian coals by nonisothermal thermogravimetry. Journal of Thermal Analysis, **37**:1161-1177.

Meng, X.L., Huang, Y.D., Yu, H. & Lv, Z.S. 2007. Thermal degradation kinetics of polyimide containing 2,6-benzobisoxazole units. Polymer Degradation and Stability, **92**:962-967.

Nazarenko, S., Meneghetti, P., Julmon, P., Olson, B.G. & Qutubuddin, S. 2007. Gas barrier of polystyrene montmorillonite clay nanocomposites: Effect of mineral layer aggregation. Journal of Polymer Science Part B: Polymer Physics, **45**:1733-1753.

Nofal, Z.M., El-Zahar, M. & Abd El-Karim, S. 2000. Novel coumarin derivatives with expected biological activity. Molecules, **5**:99-113.

Panwar, A., Choudhary, V. & Sharma, D.K. 2011. A review:polystyrene/clay nanocomposites. Journal of Reinforced Plastics and Composites, **30**:446-459.

Patonay, T., Litkei, Y.G., Bognar, R., Erdei, J. & Misztic, C. 1984. Synthesis, antibacterial and antifungal activity of 4-hydroxy-coumarin derivatives, analogues of Novobiocin. Pharmazie, **39**:86-91.

Pratibha, S. & Shreeya, P. 1999. Synthesis, Characterization and antimicrobial studies of some novel 3-arylazo-7-hydroxy-4-methylcoumarin. Indian Journal of Chemistry-Section B, **38**:1139-1142.

Shaker, R.M. 1996. Synthesis and reactions of some new 4H-pyrano[3,2-c]benzopyran-5-one derivatives and their potential biological activities. Pharmazie, **51**:148-151.

Shia, D., Hui, C.Y., Burnside, S.D. & Giannelis, E.P. 1998. An interface model for the prediction of Young's modulus of layered silicate-elastomer nanocomposites. Polymer Composites, **19**:608-617.

Soine, T.O. 1964. Naturally occurring coumarins and related physiological activities. Journal of Pharmaceutical Sciences, **53**:231-264.

Srivastava, A., Mishra, V., Singh, P. & Kumar, R. 2012. Coumarin-based polymer and its silver nanocomposite as advanced antibacterial agents: Synthetic path, kinetics of polymerization, and applications. Journal of Applied Polymer Science, **126**:395-407.

Thellen, C., Orroth, C., Froio, D., Ziegler, D., Lucciarini, J., Farrell, R., D'Souza, N.A. & Ratto, J.A. 2005. Influence of montmorillonite layered silicate on plasticized poly(L-lactide) blown films. Polymer, **46**:11716-11727.

Tian, Y., Akiyama, E., Nagase, Y., Kanazawa, A., Tsutsumi, O. & Ikeda, T. 2004. Synthesis and investigation of photophysical and photochemical properties of new side-group liquid crystalline polymers containing coumarin moieties. Journal of Materials Chemistry, **14**:3524-3531.

Vyazovkin, S. 2006. Thermal analysis. Analytical Chemistry, **78**:3875-3886.

Vyazovkin, S., Dranca, I., Fan, X. & Advincula, R. 2004. Kinetics of the thermal and thermo-oxidative degradation of polystyrene-clay nanocomposites. Macromolecular Rapid Communications, **25**:498-503.

Wang, H.W., Chang, K.C., Yeh, J.M. & Liou, S.J. 2004. Synthesis and dielectric properties of polystyrene-clay nanocomposite materials. Journal of Applied Polymer Science, **91**:1368-1373.

Wilkie, C.A. 1999. TGA/FTIR: An extremely useful technique for studying polymer degradation. Polymer Degradation and Stability, **66**:301-306.

Zanetti, M., Bracco, P. & Costa, L. 2004. Thermal degradation behaviour of PE/clay nanocomposites. Polymer Degradation and Stability, **85**:657-665.

Zhang, C.Z., Liang, R.Y., Jiang, C.X., Chen, D.B. & Zhong, A.Y. 2008. Synthesis, characterization, and self-assembly of cationic coumarin side-chain polymer. Journal of Applied Polymer Science, **108**:2667-2673.

Zhang, W.A., Chen, D.Z., Xu, H.Y., Shen, X.F. & Fang, Y.E. 2003. Influence of four different types of organophilic clay on the morphology and thermal properties of polystyrene/clay nanocomposites prepared by using the gamma-ray irradiation technique. European Polymer Journal, **39**:2323-2328.

Zhao, L., Loy, D.A. & Shea, K.J. 2006. Photodeformable spherical hybrid nanoparticles. Journal of the American Chemical Society, **128**:14250-14251.

Zidelkheir, B., Boudjemaa, S., Abdel, G.M. & Djelloui, B. 2006. Preparation and characterization of polystyrene/montmorillonite nanocomposite by melt intercalative compounding. Iranian Polymer Journal, **15**:645-653.

Zivkovic, Z.D. & Sestak, J. 1998. Kinetics and mechanism of the oxidation of molybdenum sulphide. Journal of Thermal Analysis and Calorimetry, **53**:263-267.

Submitted: 18/11/2015
Revised: 13/06/2016
Accepted: 19/06/2016